

pubs.acs.org/estengg Article

Recycling Gadolinium from Hospital Effluent via Electrochemical Aerosol Formation

Ruchiranga Ranaweera,[§] Sethma Wijesinghe,[§] Udeshika Weerarathna,[§] Aneesa Chowdhury, Aravind Babu Kajjam, Bingwen Wang, Timothy M. Dittrich, Matthew J. Allen, and Long Luo*



Cite This: https://doi.org/10.1021/acsestengg.3c00377



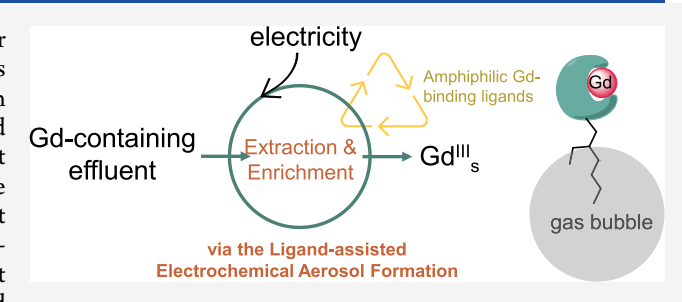
ACCESS I

III Metrics & More

Article Recommendations

Supporting Information

ABSTRACT: The increasing use of Gd-based contrast agents for magnetic resonance imaging at hospitals and research centers has led to the rapidly growing demand for Gd and Gd anomalies in surface waters. Recycling Gd from hospital effluents could simultaneously address Gd demand and severe concerns about Gd contamination. Here, we present a study relevant to the extraction and preconcentration of Gd from hospital effluents that contain parts per billion-level Gd via the ligand-assisted electrochemical aerosol formation (LEAF) process. We demonstrate that the LEAF process extracts ~75% Gd^{III} from 50 ppb Gd-spiked



water samples, including diluted artificial urine samples while preconcentrating Gd by up to 390-fold. Mechanistic studies confirm that the surface activity of the Gd-binding ligand is essential for successful LEAF extraction. The ligands are recyclable by performing electrophoretic separation in an origami paper device, followed by water extraction. The steep pH gradient and strong electric field in the origami paper device enabled the dissociation of Gd-ligand complexes, spatial separation of Gd and ligand, and precipitation of Gd^{III} as $Gd(OH)_3$. Approximately 80% of the ligands were recovered from the paper device by water extraction and reused in subsequent extraction cycles. This straightforward and green method could also be adapted to other aqueous rare earth metal wastes in the future.

KEYWORDS: rare earth element, Gd recycling, aerosol, extraction, electrophoretic separation

■ INTRODUCTION

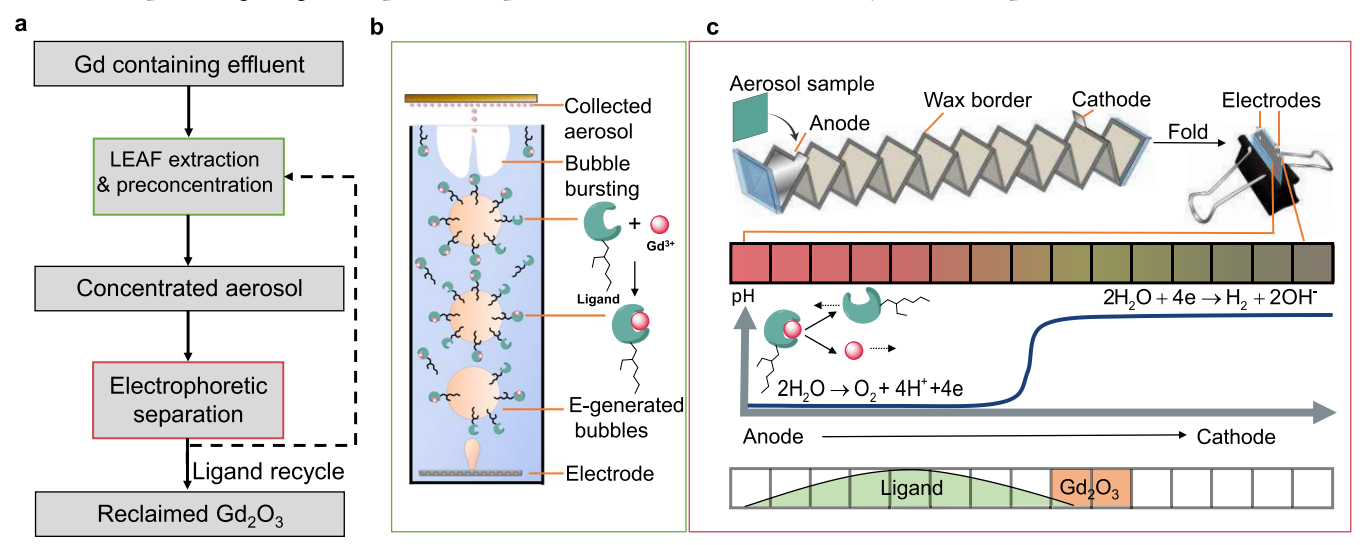
Gadolinium (Gd) is an extensively used element in contrast agents to enhance magnetic resonance imaging (MRI) signals because of the properties associated with the ⁸S_{7/2} ground state electronic configuration of Gd^{III. 1} However, because free Gd^{III} ions are toxic, the metal is used in its chelate form. Consequently, the U.S. Food and Drug Administration (FDA) and European Medicines Agency have approved several GdIII-based contrast agents that involve multidentate ligands.² Since the approval of the first Gd^{III}-based contrast agent in 1988, >450 million intravenous Gd^{III}-based contrast agent doses (approximately 1.2 g of Gd for each dose and >540 tons of Gd in total) have been administered to millions of patients worldwide.³ The global demand for Gd has been steadily increasing, reaching a market value of ~US\$5.3 billion in 2022, with a forecast to grow to US\$8.8 billion by 2032.4 The intravenously administered Gd^{III}-based contrast agents are primarily cleared via glomerular excretion with a large fraction excreted in the urine without metabolic chemical modification. In humans with normal renal function, 70% of the total injected Gd^{III} is excreted within the first urination, and more than 90% is excreted within 24 h of administration. 3,5,6 Those excreted GdIII complexes are mostly introduced into the hospital wastewater systems after application, which have

become an emerging pollutant in surface waters of great concern.⁷⁻¹⁰ The total annual Gd^{III} emission of a hospital offering a maximum spectrum of medical services was measured to be between 2.1 and 4.2 kg per year, yielding a theoretical concentration of 8.5-30.1 μ g/L or ppb in the hospital effluent. 11 GdIII chelates in hospital effluent can be transmetalated in the presence of other metal ions, such as Fe3+, ending up with free and toxic GdIII in the surface waters. 12 For example, the Gd level in surface waters collected in a transect of San Francisco Bay and their temporal variations within the Bay show a temporal increase in the Gd anomaly from 8.27 to 112 pmol/kg (or 1.3 to 17 ppt) from the early 1990s to the present. The largest Gd anomalies were observed in the San Francisco Bay region, surrounded by hospitals and research centers that use Gd^{III}-based contrast agents for MRI. Thus, recycling GdIII from hospital effluents addresses not only the rapidly increasing demand for Gd but

Revised: August 31, 2023 Revised: October 19, 2023 Accepted: October 19, 2023



Scheme 1. (a) Flowchart for Recycling Gd from Hospital Effluents; (b) Extraction and Preconcentration of Gd^{III} via the Ligand-Assisted Electrochemical Aerosol Formation (LEAF) Process; and (c) Separation of Gd^{III} from Ligand in the Collected Aerosol Sample Using Origami Paper Electrophoresis with an Electrochemically Generated pH Gradient



also growing concerns about environmental Gd contamination, both of which are of great significance and general interest to our society.

In designing a recovery system for GdIII, we started by considering current technologies for isolating GdIII. Liquidliquid or solvent extraction is the most commonly used technique for extracting and purifying rare earth elements (REEs), including Gd. 14-17 Solvent extraction involves biphasic systems composed of an organic layer doped with an extractant (or ligand) designed to bind selected REE ions from an acidic aqueous layer. However, solvent extraction consumes large volumes of high-purity solvents, producing undesired solvent wastes. 18 In addition, for environmental and economic reasons, solvent extraction is typically not directly compatible with dilute REE solutions ([REEs] < 1%) from unconventional sources—such as industrial wastes (including coal fly ash, mine tailings, and hospital effluents) and end-oflife consumer electronics (for example, electronic waste) given the challenge of REE preconcentration from these sources. 19 Another common method for REE extraction is solid-liquid extraction. Solid-liquid extraction of REEs uses a column filled with sorbent media made of solid support that serves as an attachment surface (for example, resin) and functionalized ligands that contain various functional groups for binding REEs (for example, carboxylic acids, phosphoric acids, hydroxamate, and biological ligands).^{20–23} In such systems, REEs are selectively adsorbed to the column until it is saturated, at which point a stripping solution is applied to elute the REE concentrate. This process offers several advantages relative to solvent extraction, including fast phase separation between the solid adsorbent and REE-bearing solution, reusability, and being organic-solvent-free.²³ However, one current limitation of solid-liquid extraction is the scalability.

Compared to liquid—liquid and solid—liquid extractions, gas—liquid extraction is much less investigated for recovering REE. However, gas—liquid interfaces can be more conveniently generated by gas bubble formation via water electrolysis and directly flowing gas into a liquid medium at a low cost and large scale,²⁴ relative to its liquid—liquid and solid—liquid counterparts. Here, we present a gas—liquid interface-based,

simultaneous extraction and preconcentration method for recycling parts per billion-level Gd from hospital effluents, as illustrated in Scheme 1a. First, Gd in a hospital effluent sample is extracted and preconcentrated via the ligand-assisted electrochemical aerosol formation (LEAF) process (Scheme 1b). During LEAF preconcentration, micrometer-sized gas bubbles are generated by water electrolysis. The Gd-binding ligands are engineered to be amphiphilic and spontaneously adsorb onto the gas bubble surface. As gas bubbles carrying the GdIII-binding ligands float upward, these ligands capture free Gd^{III} in solution. When bubbles burst at the surface, aerosol droplets containing GdIII-ligand complexes are released and collected. The concentration of Gd^{III} in the resulting aerosol droplets is a few hundred times greater than in the sample solution because (1) Gd^{III} accumulates on the surface of the bubbles due to the presence of GdIII-binding ligands and (2) only a thin layer of water near the bubble surface is ejected as aerosol droplets.^{24–27} The ligands in the collected aerosol droplets are recycled by electrophoretic separation of the ligand and Gd^{III} from the collected Gd^{III}-containing complexes using an origami paper-based electrophoretic device (Scheme 1c). The ligand and Gd^{III} separation rely on the electrogenerated pH gradient inside the device by water electrolysis in an unbuffered solution: acidic pH on the anode side and basic pH on the cathode side. The acidic pH demetallizes the Gd^{III}containing complex, releasing Gd^{III} from ligands, and the metal ion and ligand are electrophoretically separated from each other under the strong (10 to 20 kV/m) electrical field. As Gd^{III} migrates toward the cathode, the ions experience an increase in pH and, consequently, precipitate as GdIII hydroxides on the paper, achieving the spatial separation of Gd^{III} from the ligand. The ligand on the paper is recovered by dissolution in an aqueous solution and reused for the next extraction cycle.

As proof of concept, we demonstrate the extraction of up to 75% Gd in 2 h from water and diluted artificial urine samples containing 50 ppb Gd^{III} (the Gd level in the wastewater of MRI imaging hospitals) via the LEAF process. The Gd and ligand are completely separated using an origami paper-based electrophoresis device. Gd is obtained as $Gd(OH)_3$, where the

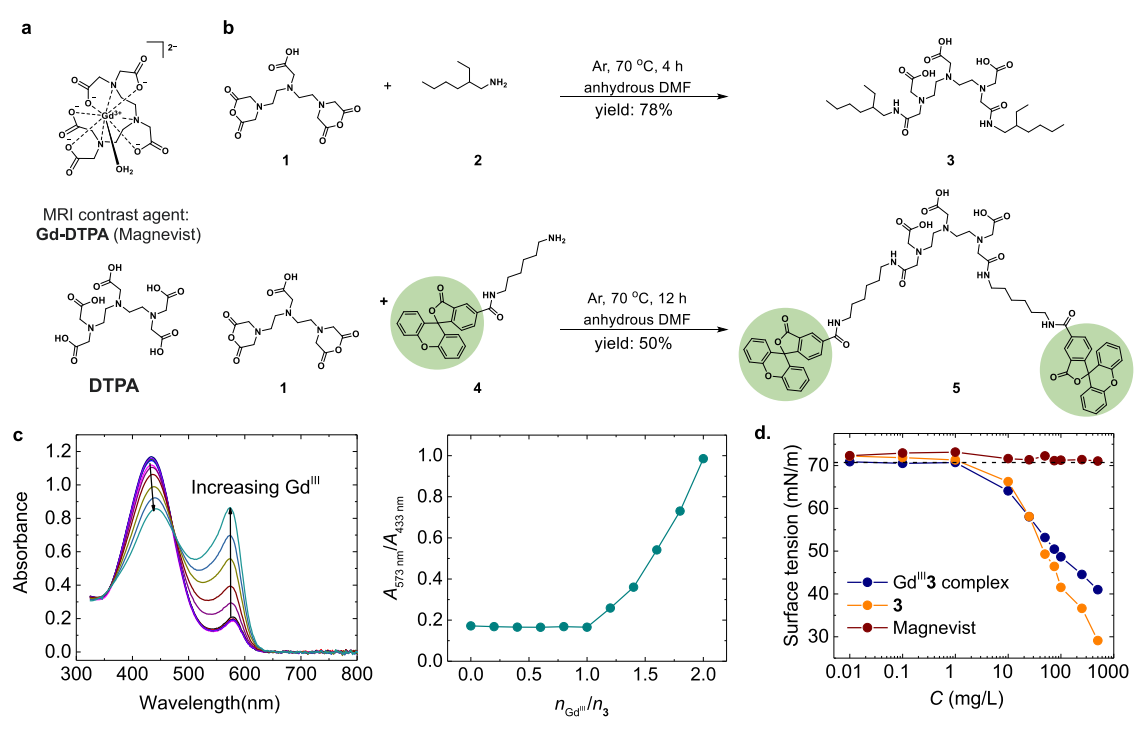


Figure 1. Synthesis and characterization of amphiphilic Gd-binding ligands. (a) Molecular structures of Magnevist and its ligand DTPA. (b) Synthesis of amphiphilic bis(ethylhexyl)amido DTPA, 3, and a fluorescein-labeled version of the ligand, 5. (c) Complexometric titration data for determining the stoichiometry of the complexation reaction between Gd^{III} and 3. Left: UV–visible spectra of a mixture of 3 (0.25 μ mol), varied amounts of Gd^{III}, and Xylenol orange in an acetic buffer solution (pH = 5.8, total volume = 12 mL). Right: ratio of absorbances at 573 and 433 nm as a function of the molar ratio of Gd^{III}/3 ($n_{\rm Gd}/n_3$). (d) Surface tensions of Magnevist, 3, and Gd^{III}3 solutions as a function of concentration. DMF: dimethylformamide.

ligand is recovered from the paper device by a water extraction step with an extraction efficiency of ~80%. Our proof-of-concept study demonstrates a highly novel approach to addressing the increasing demand for Gd while solving the environmental problem caused by the growing use of Gd-based MRI contrast agents; both are of great significance and general interest. This straightforward and green protocol could also be adapted to other aqueous metal wastes in the future.

■ RESULTS AND DISCUSSION

Synthesis and Characterization of Amphiphilic Gd^{III}-Binding Ligands. Diethylenetriaminepentaacetic acid (DTPA) is the ligand used in the first GdIII-based contrast agent approved by the U.S. Food and Drug Administration: [Gd(H₂O)(DTPA)]²⁻ (trade name: Magnevist, Figure 1a).²⁸ The complexation equilibrium constant of GdIII and DTPA is 10^{22} at pH = 7, about ten times stronger than Cu^{II} and 10^4 times stronger than Zn^{II}. ²⁹ In this study, we synthesized an amphiphilic GdIII-binding ligand 3 by installing two hydrophobic ethylhexyl groups on the DTPA backbone (3 in Figure 1b) following a reported procedure.³⁰ Briefly, a solution of ethylhexylamine 2 in anhydrous dimethylformamide under an atmosphere of Ar was heated to 70 °C. Diethylenetriaminepentaacetic bis-anhydride, 1, was added to the solution while stirring. The reaction mixture was stirred for 4 h at 70 °C. Solvent was removed under reduced pressure, and the resulting light-yellow oil was solidified by adding acetone. The solid was recrystallized from boiling ethanol to yield 3 as a white microcrystalline solid. We also synthesized a fluoresceinlabeled version of the ligand, 5, that we used to study the electrophoretic separation of Gd^{III} from the ligand after extraction. Ligand 5 was synthesized following a similar

method as for the synthesis of 3 but with fluorescein amine 4 at a prolonged reaction time of 12 h. The product was recrystallized from boiling ethanol to yield 50% 5 as a yellowish-orange crystalline solid. The identity and purity of 3 and 5 were characterized using $^{1}\text{H-}$ and ^{13}C NMR spectroscopy and mass spectrometry (Figures S1–S4).

Next, we measured the stoichiometry of the complexation reaction between GdIII and 3 using a reported complexometric titration protocol.³¹ Briefly, Xylenol orange was added to a solution of 3 as an indicator during the titration experiment. In the presence of free Gd^{III} in solution, Xylenol orange changes color from yellow to violet because coordination of Gd^{III} with Xylenol orange results in an extended electronic delocalization. Figure 1c shows the UV-visible spectra of solutions of 3 and Xylenol orange after adding increasing amounts of Gd^{III}. The free Gd^{III} concentration is directly proportional to the ratio of the absorbances at 573 and 433 nm (A_{573}/A_{433}) . At Gd^{III}/3 molar ratios (n_{Gd}/n_3) < 1, A_{573}/A_{433} shows no apparent difference, but it increases nearly linearly with $n_{\rm Gd}/n_3$ at $n_{\rm Gd}/n_3$ > 1. The complexometric titration result indicates that 3 binds with GdIII at a stoichiometric ratio of 1, the same ratio observed with DTPA. We then measured the surface tensions of Magnevist, Magnevist 3, and GdIII3 solutions. Figure 1d shows the solution surface tension (γ) starts decreasing at 1 mg/L of 3 and Gd^{III}3 with a nearly linear relationship between γ and log(concentration) from 10 mg/L to 1 g/L. The nearly linear dependence of γ on log(concentration) is typical for surfactants. The $Gd^{III}3$ complex shows a slightly lower γ than that of 3 alone. In contrast, Magnevist shows no surface activity.

Gd Extraction from Gd-Spiked Water. With the amphiphilic Gd^{III}-binding ligand in hand, we performed the

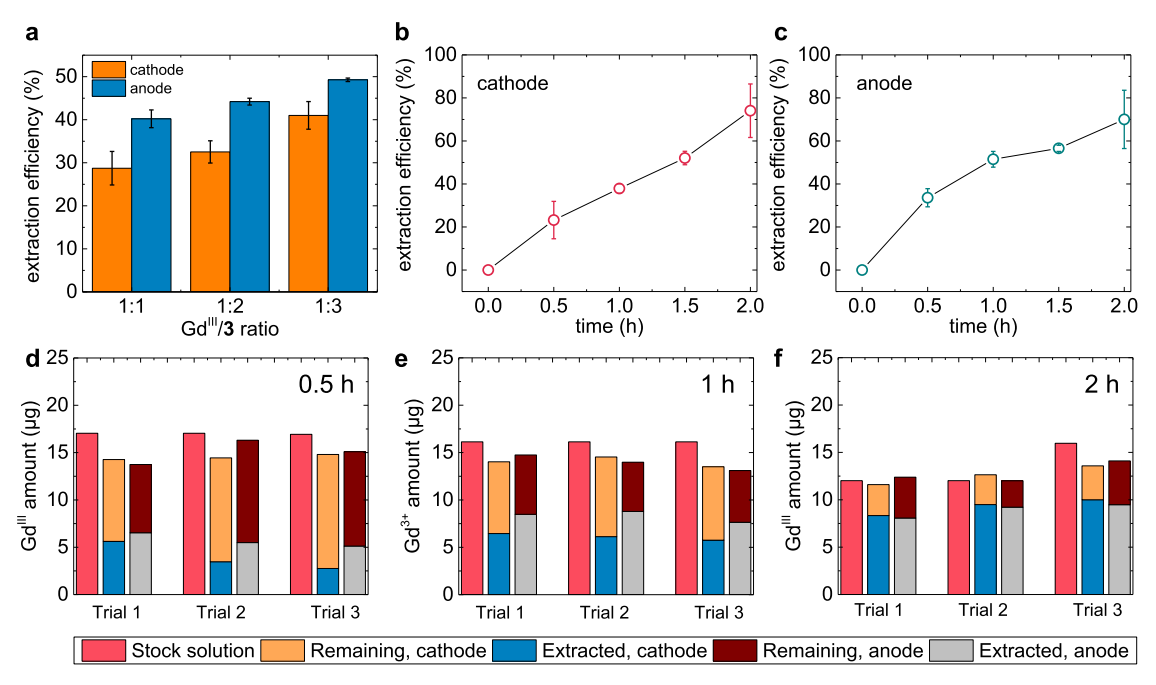


Figure 2. Extraction of Gd from Gd-spiked water. (a) Efficiencies of Gd extraction at the cathode (orange) and anode (blue) using different ratios of Gd^{III} and 3 after 1 h of the LEAF extraction process. Extraction efficiency as a function of the extraction time at the (b) cathode and (c) anode at a molar ratio between Gd^{III} and 3 of 1:3. (d)–(f) Mass balance analysis of Gd content before and after the LEAF extraction at different extraction times of 0.5, 1, and 2 h. In all experiments, the initial concentration of Gd^{III} was 50 ppb.

LEAF extraction using an experimental apparatus similar to our previous studies of the preconcentration of per- and polyfluoroalkyl substances.^{27,32} Specifically, a home-built Htype cell was made of two polypropylene graduated cylinders to accommodate a total solution volume of 650 mL (Figure S5). Two nickel foam electrodes (2.5 cm² each) were separately immersed in the two cylinders and used as the anode and cathode to promote bubble generation via water electrolysis. As shown in Scheme 1B, GdIII and free 3 should spontaneously attach to these bubbles' gas-liquid interface due to their amphiphilicity. As the bubbles arrive at the solution surface, they burst and produce aerosol droplets enriched with the Gd^{III}3. The droplets are collected by a glass slide and transferred into a volumetric flask to quantify Gd using an inductively coupled plasma mass spectrometer (ICP-MS).

Our sample solutions contained $GdCl_3$ (50 ppb), 3 (1 to 3 equiv relative to Gd^{III}), and NH_4HCO_3 (0.2 M) as the supporting electrolyte. We chose NH_4HCO_3 for the following reasons: First, the pH of the solution is 8.4, so the carboxylic acids of 3 are fully deprotonated to enable chelation of Gd^{III} . 30,33 Second, NH_4HCO_3 reacts with in situ generated H^+ at the anode during water electrolysis to produce a mixture of CO_2 and O_2 gas. The generation of CO_2 gas increases the total volumetric gas flux and provides a larger liquid/gas interface, relative to electrolytes that do not form CO_2 gas, to facilitate the interaction between Gd^{III} and 3, thus improving the extraction efficiency.

We first evaluated the effect of the Gd^{III} /ligand ratio on the extraction efficiency. Figure 2a shows that the efficiency of Gd^{III} extraction after 1 h of the LEAF process reached $40 \pm 2\%$ for the anodic compartment and $29 \pm 4\%$ for the cathodic compartment at a $Gd^{III}/3$ ratio of 1:1. The greater extraction efficiency at the anode is expected because of the larger gas flux at the anode than at the cathode (the theoretical volumetric

gas flux ratio between the anodic and cathodic sides is 2.5:1). A mixture of O2/CO2 from water oxidation and the reaction between H⁺ and HCO₃⁻ contributes to the anodic gas flux while H2 generated from water reduction contributes to the cathodic gas flux. Changing the ratio of GdIII/3 to 1:3 improved the extraction efficiency, to 49 \pm 1% at the anode and $41 \pm 3\%$ at the cathode. The ratio of extraction efficiencies between the anodic and cathodic compartments is lower than the corresponding ratio of electrogenerated gas flux because the total gas/liquid surface available for ligand adsorption is not proportional to the gas flux. The initial CO_2/O_2 bubble size at the anodic compartment is about 20% larger than the H₂ bubble at the cathodic compartment. Then, due to the CO₂ dissolution, the anodic bubble size shrinks to ~50% of the cathodic bubbles as they float upward.³² Thus, the total gas/ liquid surface available for ligand adsorption on the anodic side is initially two times and then decreased to ~40% of the cathodic one, leading to a lowered ratio of extraction efficiency at the anode.

Further, the extraction efficiency increases with time, reaching 76 \pm 7% at the cathode and 72 \pm 9% at the anode after 2 h of LEAF extraction at a GdIII/3 ratio of 1:3 (Figure 2b-c). The total volume of collected aerosol droplets is approximately 1.5 mL on the cathode side and 0.6 mL on the anode side, yielding ~160- and 390-fold Gd preconcentration relative to the initial sample solution on the cathode and anode sides, respectively. We also performed a mass balance analysis for Gd before and after the LEAF extraction. Figure 2d-f shows the measured amounts of Gd in the stock solution before LEAF extraction (red), remaining in the cathodic (orange) and anodic (wine) compartments after the extraction, and extracted as aerosol droplets (blue and gray) for three repeated experiments. We successfully recovered ~87 to 96% of the initial Gd in the system. The slight loss of Gd during LEAF extraction may be due to the imperfect collection of

aerosol droplets. As a control, we ran the LEAF extraction of Magnevist but did not observe noticeable (<2%) extraction due to no significant accumulation of Magnevist at the gas/liquid interface of gas bubbles (Figure S6), indicating that the amphiphilicity of the Gd^{III}-binding ligand is essential to the success of the LEAF extraction.

To confirm that 3 extracts Gd^{III} , we performed liquid chromatography—mass spectrometry (LC-MS) analysis of free 3 in the collected aerosol droplets. The chromatograms and calibration curves for free 3 in aqueous NH_4HCO_3 (0.2 M) are provided in Figure S7. The neutral $Gd^{III}/3$ complex cannot be ionized under standard electrospray ionization conditions and is thus not detected by LC-MS (Figure S7). The LC-MS analysis of the collected aerosol droplets shows that nearly all of 3 is in the form of the LC-MS-silent neutral complex (Figure S8), consistent with Gd^{III} ions being extracted by 3 attached to the surface of the electrogenerated gas bubbles.

Gd Extraction from Diluted Artificial Urine Samples. Next, we tested the feasibility of extracting and preconcentrating Gd^{III} from diluted artificial urine samples that simulate GdIII-containing hospital wastewater. We prepared artificial urine according to the formula of Shmaefsky: 34 urea (18.2 g/ L), NaCl (7.5 g/L), KCl (4.5 g/L), and Na₃PO₄ (4.8 g/L) were dissolved in water followed by pH adjustment to 5 with aqueous HCl. The artificial urine solution was diluted by a factor of 12 to simulate the dilution during toilet flush (the volume of urine passed each time by a normal adult varies from around 250 to 400 mL, and toilet flush volumes vary from 4 to 6 L). The diluted artificial urine sample was spiked with 50 ppb GdCl₃ and 3 equiv of 3. NH₄HCO₃ was added to achieve a final concentration of 0.2 M. The molar ratio of Gd^{III} to 3 was 1:3. Figure 3a shows that the Gd^{III} extraction efficiency after 1 h of the LEAF extraction is ~60% for three independent trials,

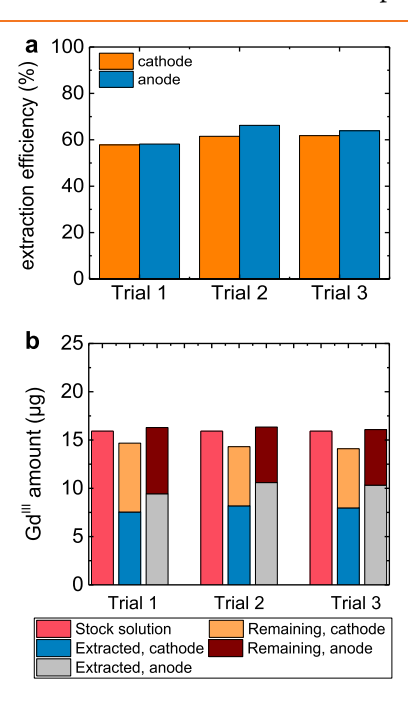


Figure 3. Extraction of Gd^{III} from diluted artificial urine. (a) Gd^{III} extraction efficiencies at the cathode (orange) and anode (blue) from diluted artificial urine samples containing Gd^{III} (50 ppb) after 1 h of the LEAF extraction process at 0.2 A. The molar ratio of Gd^{III} to 3 is 1:3. (b) Mass balance analysis of the Gd content before and after LEAF extraction.

similar to that for water samples in Figure 2. This result indicates that low concentrations of urea, NaCl, KCl, and Na₃PO₄ had no adverse effects on the extraction process. The similar extraction efficiencies between the anode and cathode might be caused by the presence of Na₃PO₄, which can act as a buffer to reduce the level of CO₂ generation at the anode. Additionally, the Gd mass balance analysis in Figure 3b shows no significant loss of Gd during the extraction process.

Separation of Gd^{III} from Ligand Using Paper Electrophoresis. After the successful extraction and preconcentration of GdIII3, we explored the reusability of the system using origami paper electrophoresis to separate 3 from Gd^{III} in the form of Gd₂O₃ (one of the most commonly available forms of Gd). The device fabrication and operation methods are detailed in the Experimental Section and in Figure S9. Briefly, the wax-patterned chromatography paper was wetted with KNO₃ (100 mM) and folded into 20-layer origami (Scheme 1c). Then, two Pt electrodes were inserted between layers 1 and 2 (anode) and between layers 19 and 20 (cathode). The aerosol sample containing GdIII3 was introduced onto a piece of filter paper with the exact dimensions as the other paper layers of the device and placed between layers 2 and 3. Finally, the folded paper and the electrodes were sandwiched between two acrylic sheets and clamped using a binder clip to ensure good contact between different layers and ensure device rigidity.

The separation of Gd^{III} from 3 was initiated by applying a voltage bias of 50 V between the two Pt electrodes. Water oxidation in a KNO3 aqueous solution generates a strong acid (HNO₃) at the anode, whereas water reduction in the same solution generates a strong base (KOH) at the cathode. Pt electrodes were used to handle extreme pHs at the cathode and anode. Thus, the voltage creates a large pH gradient inside the origami paper device. Figure 4a shows that the pH value is \sim 1 on layers 2–12, transitions to nearly neutral on layer 13, and remains slightly basic beyond layer 14. According to Benazeth's X-ray absorption study on the dissociation of Gd^{III}DTPA,³⁵ Gd^{III}DTPA dissociates in the pH range of 0.15 to 1.5. Compared to GdIIIDTPA, GdIII3 is less stable and dissociates at pH < 3.5.30 The difference between DTPA and 3 is due to two carboxylate groups of DTPA being replaced with amides in 3. Ligand 3 released from the dissociation of Gd^{III}3 is protonated by up to 5 H⁺ to form H_53^{2+} cations at pH = \sim 1: three on carboxylate groups and two on amines (the equilibrium constant for $H_5 \tilde{3}^{2+}/H_4 3^+$ is ~ 0.7). The GdIII and protonated 3 are electrophoretically separated from each other based on the difference in their mobility, driven by the strong electric field in the origami paper device. Due to the thinness of the device (\sim 3 mm), a strong electric field of \sim 16 kV/m is generated with merely 50 V.^{37,3}

To visualize the separation of Gd^{III} from 3, we used fluorescent ligand 5 (absorption and emission spectra are shown in Figure S10). We added a mixture of Gd^{III} and 5 (molar ratio of 1:1) to the origami paper device in an amount that matches a 75% extraction efficiency. After running the separation for 3 min at 50 V, the paper device was disassembled, and the origami paper was unfolded and analyzed using an energy-dispersive X-ray fluorescence spectrometer for Gd quantification and a macro view fluorescence microscope for quantification of 5. Because the fluorescence intensity of 5 is pH-dependent (Figure S11), the paper layers were neutralized by phosphate buffer (100 mM, pH = 7.0) before fluorescence imaging. Figure 4b,c shows the

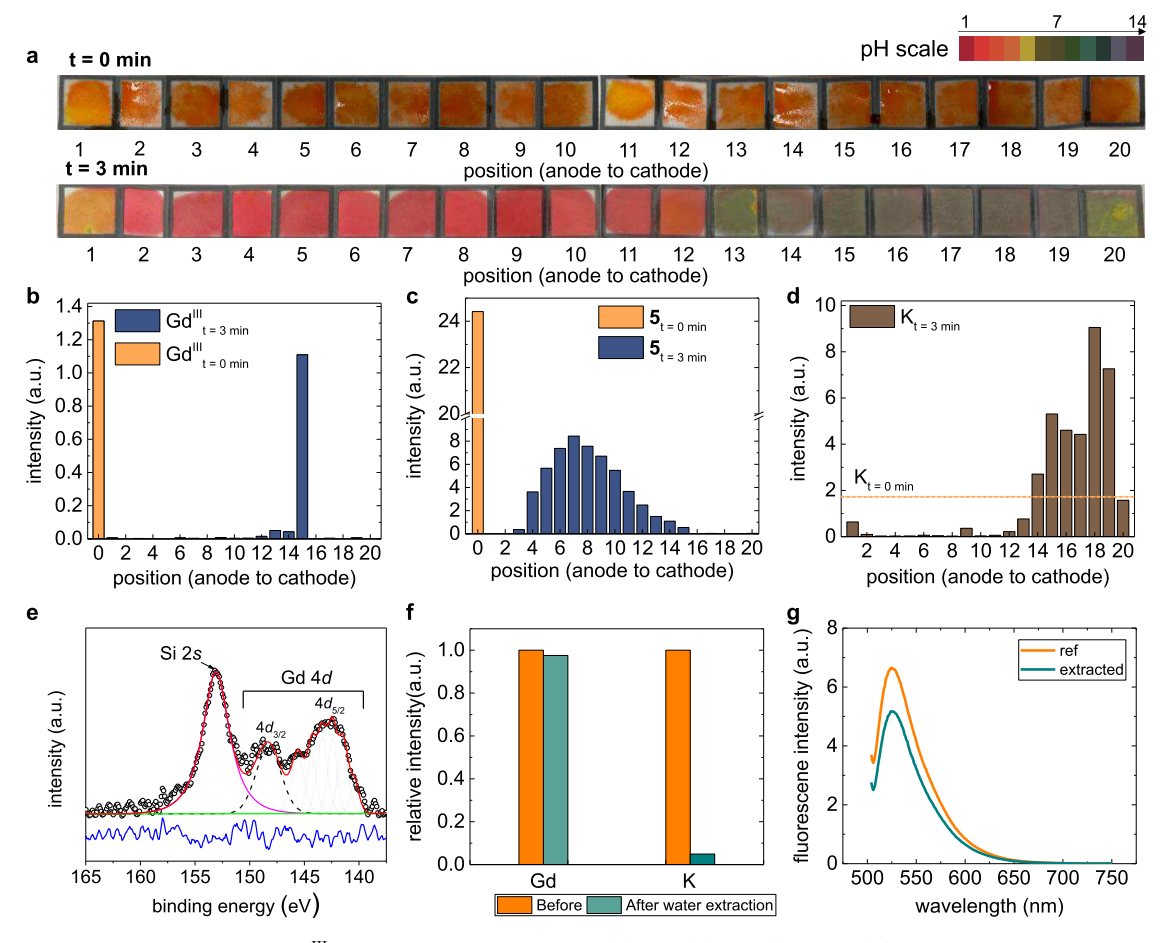


Figure 4. Electrophoretic separation of Gd^{III} from ligand. Distributions of (a) pH, (b) Gd, (c) **5**, and (d) K on the different layers of an origami paper device before and after a 3 min electrophoretic separation at 50 V. A universal pH indicator solution was used to indicate the pH environment on each paper layer. (e) X-ray photoelectron spectroscopy results of the Gd 4*d* region for layer 15 after separation. Black circles: experimental data; green line: background; red curve: fitted data; blue curve: residual plot. (f) Comparison of Gd and K contents on layer 15 before (orange bar) and after (green bar) water extraction. (g) Fluorescence intensity of the extracted **5** solution (green) and the reference solution (orange). Excitation wavelength = 494 nm. The sample pH was adjusted to 7 before fluorescence measurements.

distributions of Gd^{III} and 5 in the origami paper device after separation for 3 min at 50 V (blue bars). The signal intensities of total Gd and 5 before separation are provided as references (orange bars, layer 0). Nearly all Gd localized on layer 15, and 5 exhibited a Gaussian distribution from layer 3 to 15. The Gaussian distribution of 5 is expected because of the diffusional motion of 5 during electrophoresis. The diffusivity of 5 in a wet paper (D_5) can be roughly estimated to be $\sim 0.4 \times 10^{-9}$ m²/s using the one-dimensional Einstein diffusion equation (eq 1),

$$\Delta \sigma^2 = 2D_5 t \tag{1}$$

where $\Delta\sigma^2$ is the mean-square displacement at time t ($\sigma=2.63$ layers or 0.4 mm at t=3 min, Figure S12). The D_5 value is comparable to the diffusivity of other fluorescent molecules in wet filter paper (for example, \sim 0.14 \times 10⁻⁹ m²/s for BODIPY²-). However, this diffusion model does not explain the highly localized distribution of Gd on layer 15 that should be caused by the precipitation of Gd in the paper device is at the 10-ppm level or \sim 60 μ M. Because the $K_{\rm sp}$ of Gd(OH) $_3$ is \sim 10⁻¹⁸, 39 Gd^{III} should start precipitating at pH \approx 9.4, consistent with the slightly alkaline environment on layer 15. In comparison, we analyzed the distribution of another cation,

 $\rm K^+$, in this electrophoresis system that also electromigrated to the cathode but does not precipitate at basic pH values. We observed the broad distribution of $\rm K^+$ on layers 12 to 20 (Figure 4d), supporting the precipitation mechanism for $\rm Gd^{III}$. We also conducted an X-ray photoelectron spectroscopy analysis of the separated Gd (Figure 4e). The Gd 4d region shows one peak for $\rm 4d_{3/2}$ at ~ 148 eV and another broad peak for $\rm 4d_{5/2}$ at ~ 142 eV. The peak fitting provides a single-peak fit for the 148 eV peak but multiplets for the 142 eV peak, consistent with the X-ray photoelectron spectroscopy results of Gd 4d region of $\rm Gd(OH)_3$. The broad multiplet structure arises from the interactions between the angular momentum of the $\rm ^8S_{7/2}$ state of the half-filled $\it f$ shell and the total angular momentum of the 4d core hole of $\rm Gd^{III}$.

The steep pH gradient and strong electric field in the origami paper device enabled the spatial separation of Gd^{III} from 5 onto different paper layers. To reclaim 5, we washed the filter paper with water to extract 5, leaving Gd on the paper due to the poor solubility of $Gd(OH)_3$ in water. Figure 4f shows that nearly all Gd remained on layer 15, and ~95% of K was removed from this layer. The peak fluorescence intensity of the extract after extracting 5 from layers 1–13 using ultrapure water (3 × 10 mL) is ~80% of the peak intensity for a reference sample with the total starting amount of 5 (Figure 4g). A similar extraction efficiency of 82% from filter paper was

achieved for the nonfluorescent 3. The loss of 20% ligands during water extraction is possibly caused by the nonspecific adsorption of 5 onto the cellulose fibers of filter paper, a small amount of photobleaching, or both adsorption and photobleaching. The recycled $Gd(OH)_3$ can be converted to Gd_2O_3 by burning the Gd-loaded filter paper in a furnace, and the reclaimed 3 is available for reuse in another cycle of the Gd^{III} extraction process.

SUMMARY AND CONCLUSIONS

We performed a proof-of-concept study relevant to extracting and preconcentrating Gd^{III} from hospital effluent that contains ppb-level Gd^{III} via the ligand-assisted electrochemical aerosol formation (LEAF) process (Figure 5). We demonstrated that

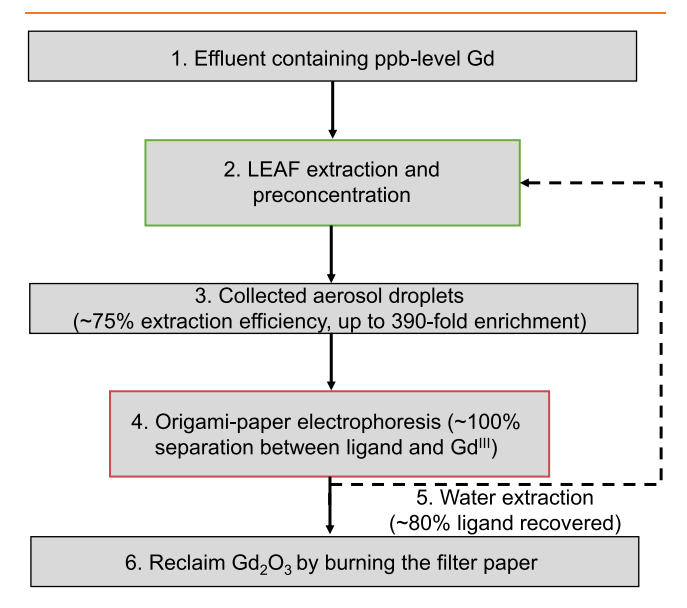


Figure 5. Performance of the proposed workflow for recycling Gd^{III} from hospital effluent.

the LEAF process extracted ~75% Gd^{III} from water samples, including diluted artificial urine samples, spiked with 50 ppb Gd that preconcentrates Gd^{III} by up to 390-fold. Mechanistic studies confirmed that the surface activity of the Gd^{III}-binding ligand is essential to the success of LEAF extraction. The ligands are recyclable by performing electrophoretic separation in an origami paper device followed by water extraction. The steep pH gradient and strong electric field in the origami paper device enable the dissociation of GdIII from ligands, spatial separation of Gd^{III} from the ligand, and precipitation of Gd^{III} as Gd(OH)₃. Roughly 80% of the ligands were recovered from the paper device by water extraction to be reused in the next run. Gd(OH)₃ on paper can be easily converted to Gd₂O₃ by a thermal treatment. Our proposed workflow is simple and environmentally friendly without using organic solvents, columns, and expensive equipment: the input is electricity and Gd^{III}-containing water; the output is Gd₂O₃ and gases (H₂, O2, and CO2); and the GdIII-binding ligand and electrolytes (KNO₃ and NH₄HCO₃) are recyclable. The amount of Gd extracted through our system in this work was at the microgram scale, making it difficult to assess the product purity and ligand reusability. Currently, we are working on scaling up the reaction setup to handle real-world hospital effluent samples. We expect the successful recycling of Gd^{III} from hospital effluent will address the rapidly increasing

demand for Gd^{III} and solve the growing environmental Gd^{III} contamination problem.

■ EXPERIMENTAL SECTION

Chemicals and Materials. Ammonium bicarbonate (99%), gadolinium chloride hexahydrate (99%), gadolinium standard for ICP (TraceCERT), potassium nitrate (99%), potassium dihydrogen phosphate (99%), disodium hydrogen phosphate (99%), nitric acid (67–70%), xylenol orange tetrasodium salt, acetic acid (99.7%), and Whatman cellulose chromatography papers 1 Chr sheets (20 × 20 cm) were purchased from Sigma-Aldrich. Ethylhexylamine (>98.0%) and diethylenetriaminepentaacetic bis-anhydride (>98%) were purchased from TCI Chemicals and used as purchased. Nickel Foams (200 mm × 300 mm × 1.0 mm) were purchased from Amazon (Brand = Futt). Ultrapure water (18 M Ω cm, total organic carbon <3 ppb) was used in all aqueous solutions.

Synthesis of Gd^{III}-Binding Ligands. Bis(ethylhexyl)-amido diethylenetriaminepentaacetic acid (3): Ligand 3 was prepared following a reported procedure.³⁰ A solution of ethylhexylamine (2.73 g, 7.66 mmol) in anhydrous dimethylformamide (50 mL) under an atmosphere of Ar was heated to 70 °C. Diethylenetriaminepentaacetic bis-anhydride (2.000 g, 15.47 mmol) was added to the solution while stirring. The reaction mixture was stirred for 4 h at 70 °C. Solvent was removed under reduced pressure, and the resulting light-yellow oil was solidified by adding acetone (30 mL). The solid was recrystallized from boiling ethanol to yield 3.6 g (78%) of 3 as a white microcrystalline solid.

12,15-Bis(carboxymethyl)-1,10-dioxo-1-(3-oxo-3H-spiro-[isobenzofuran-1,9'-xanthen]-5-yl)-18-((6-(3-oxo-3H-spiro-[isobenzofuran-1,9'-xanthene]-5-carboxamido)hexyl)-carbamoyl)-2,9,12,15,18-pentaazaicosan-20-oic acid (5). A solution of fluorescein amine, 5-isomer (250 mg, 0.49 mmol) in anhydrous dimethylformamide (15 mL) under an atmosphere of Ar was heated to 70 °C. Diethylenetriamine-pentaacetic acid bis-anhydride (86 mg, 0.24 mmol) was added to the solution while stirring. The reaction mixture was stirred for 12 h at 70 °C. Solvent was removed under reduced pressure, and the resulting orange oil was solidified by adding acetone (15 mL). The solid was recrystallized from boiling ethanol to yield 302 mg (50%) of 5 as a yellowish-orange crystalline solid. Characterization data are provided as Figures S1–S4.

LEAF Extraction. All experiments were performed using a home-built H-type two-compartment electrochemical cell. The cell was filled with 650 mL of aqueous ammonium bicarbonate (0.2 M, pH = 8.4), Gd^{III}, and ligands. Two Ni foam electrodes (2.5 cm² each) were separately immersed into the two compartments and used as the anode and cathode. A constant current of 0.2 A was applied between the two electrodes. The aerosol droplets produced by bubble bursting were collected by using glass slides placed 3 mm above the liquid surface. The aerosol droplets were collected using a micropipette every \sim 20 min and transferred to a 10 mL volumetric flask. At the end of the LEAF extraction, the glass slide was washed with deionized water to collect all of the remaining Gd^{III} on the slide.

Origami Paper Device Fabrication. Cellulose chromatography paper was used for paper device fabrication. First, 20 square strips (1 cm²) were printed using a Xerox ColorQube 8580 wax printer. Next, the printed paper was heated using a hot plate, setting the temperature at 130 °C to enable wax to penetrate the paper. Paper panels were folded as shown in

Scheme 1, and Pt electrodes were placed on two ends of the paper device. Two acrylic plastic sheets were used as the two ends

Complexometric Titration. A sample of aqueous Gd (5.0 mL of 0.001 M) and acetic acid buffer (10.00 mL, pH 5.8) was combined in a glass flask. Ultrapure water was added to adjust the final volume to 30.0 mL. A few drops of Xylenol orange were added to the flask. The resulting solution was titrated with an aqueous solution (0.1 mM) of 3. A color change from violet to yellow was observed during the titration. UV—visible spectra were recorded using a Thermo Scientific GENESYS 50 UV—vis spectrophotometer.

ICP-MS Analysis. ICP-MS measurements were performed on an Agilent Technologies 7700 series spectrometer. All samples were diluted to the proper concentration for ICP-MS measurements with 5% $\rm HNO_3$, which was also used as the blank during calibration. The calibration curve was created for a concentration range of 0.1–150 ppb (diluted from a 1000 ppm ICP standard solution). All samples were heated for 12 h at 70 $^{\circ}$ C for acid digestion before the analysis.

LC-MS Analysis. All LC-MS experiments were performed using a Shimazu LCMS-8040 Liquid Chromatograph Mass Spectrometer equipped with a Nexera X2 LC-30AD solvent delivery unit, triple quadrupole mass analyzer, Prominence CTO-20AC column oven, and a Nexera SIL-30AC MP autosampler. All experiments were performed in negative ionization and multiple reaction monitoring (MRM) modes. 50 μ L of aliquots of sample extracts was injected into an analytical column (Waters Symmetry C18 (4.6 mm × 77 mm × 3.5 mm)). A gradient of aqueous ammonium acetate (20 mM) (solvent A) and acetonitrile (solvent B) was used for the elution procedure: 0–1 min, 20% B; 1–5 min, 75% B; 5–5.1 min, 100% B; 5.1–6 min, 100% B. The flow rate was 0.4 mL min⁻¹, and the temperature of the analytical column was maintained at 30 °C.

Fluorescence Analysis. Paper electrophoresis was performed using a 20-layer origami paper device at 50 V for 3 min with aqueous KNO₃ (100 mM) as an electrolyte solution, and the pH was adjusted to 7 before fluorescence analysis. Fluorescence images of each paper layer were acquired using an Olympus MVX10 Macro Zoom Fluorescence Microscope System with a U-MGFPHQ/XL Fluorescence Filter Cube. For the water extraction efficiency analysis, we used a different protocol. First, the first 13 paper layers counting from the anode side were placed into a 50 mL centrifuge tube. Ligand 5 that was adsorbed on these layers was extracted with ultrapure water $(3 \times 10 \text{ mL})$, and the combined extracts were diluted to 50.0 mL with ultrapure water. An aliquot (400 μ L) of the resulting solution was transferred into a 50.0 mL volumetric flask and filled to the mark using ultrapure water. The fluorescence intensity of the solutions was measured using a JASCO FP-6500 spectrofluorometer with an excitation wavelength of 494 nm.

X-ray Photoelectron Spectroscopy and Energy-Dispersive X-ray Fluorescence Spectrometry Analysis. A Thermo Scientific Nexsa Surface Analysis System and a Shimadzu EDX-7000 energy-dispersive X-ray fluorescence spectrometer were directly used to analyze Gd on the paper layers.

ASSOCIATED CONTENT

Supporting Information

The Supporting Information is available free of charge at https://pubs.acs.org/doi/10.1021/acsestengg.3c00377.

Characterization data (including NMR spectra and mass spectrometric data) for 3 and 5, photographs of the home-built LEAF apparatus and origami paper electrophoresis device, LEAF extraction and preconcentration of Magnevist, LC-MS analysis of solutions of 3 and Gd^{III}3, absorption and emission spectra of 5, pH-dependent fluorescence intensity of 5, and Gaussian fitting of the distribution of 5 in the paper device (PDF)

AUTHOR INFORMATION

Corresponding Author

Long Luo – Department of Chemistry, Wayne State University, Detroit, Michigan 48202, United States; orcid.org/0000-0001-5771-6892; Email: long.luo@ wayne.edu

Authors

Ruchiranga Ranaweera - Department of Chemistry, Wayne State University, Detroit, Michigan 48202, United States Sethma Wijesinghe – Department of Chemistry, Wayne State University, Detroit, Michigan 48202, United States Udeshika Weerarathna – Department of Chemistry, Wayne State University, Detroit, Michigan 48202, United States Aneesa Chowdhury – Department of Chemistry, Wayne State University, Detroit, Michigan 48202, United States Aravind Babu Kajjam - Department of Chemistry, Wayne State University, Detroit, Michigan 48202, United States Bingwen Wang - Department of Chemistry, Wayne State University, Detroit, Michigan 48202, United States **Timothy M. Dittrich** – Department of Civil and Environmental Engineering, Wayne State University, Detroit, Michigan 48202, United States Matthew J. Allen - Department of Chemistry, Wayne State University, Detroit, Michigan 48202, United States; orcid.org/0000-0002-6868-8759

Complete contact information is available at: https://pubs.acs.org/10.1021/acsestengg.3c00377

Author Contributions

§R.R., S.W., and U.W. contributed equally to this work. The manuscript was written through the contributions of all authors. All authors have given approval to the final version of the manuscript.

Notes

The authors declare no competing financial interest.

ACKNOWLEDGMENTS

The authors acknowledge support from the National Science Foundation under award CHE-1943737 and the United States Army Engineer Research and Development Center (ERDC) under Cooperative Agreement Number W912HZ-21-2-0048. This work used the UPS/XPS partially funded by the National Science Foundation #1849578, and the NMR spectrometer partially funded by the National Institutes of Health (1S10OD028488-01A1)

REFERENCES

- (1) Caravan, P.; Ellison, J. J.; McMurry, T. J.; Lauffer, R. B. Gadolinium(III) chelates as MRI contrast agents: Structure, dynamics, and applications. *Chem. Rev.* **1999**, *99* (9), 2293–2352.
- (2) Rogosnitzky, M.; Branch, S. Gadolinium-based contrast agent toxicity: a review of known and proposed mechanisms. *BioMetals* **2016**, 29 (3), 365–376.
- (3) McDonald, R. J.; Levine, D.; Weinreb, J.; Kanal, E.; Davenport, M. S.; Ellis, J. H.; Jacobs, P. M.; Lenkinski, R. E.; Maravilla, K. R.; Prince, M. R.; Rowley, H. A.; Tweedle, M. F.; Kressel, H. Y. Gadolinium Retention: A Research Roadmap from the 2018 NIH/ACR/RSNA Workshop on Gadolinium Chelates. *Radiology* **2018**, 289 (2), 517–534.
- (4) Gadolinium Market Overview (2022–2032). https://www.futuremarketinsights.com/reports/gadolinium-market (accessed Oct 19, 2023).
- (5) Loreti, V.; Bettmer, J. Determination of the MRI contrast agent Gd-DTPA by SEC-ICP-MS. *Anal. Bioanal. Chem.* **2004**, *379* (7–8), 1050–1054.
- (6) Weinmann, H. J.; Brasch, R. C.; Press, W. R.; Wesbey, G. E. Characteristics of gadolinium-DTPA complex: a potential NMR contrast agent. *AJR*, *Am. J. Roentgenol.* **1984**, 142 (3), 619–624.
- (7) Rogowska, J.; Olkowska, E.; Ratajczyk, W.; Wolska, L. Gadolinium as a new emerging contaminant of aquatic environments. *Environ. Toxicol. Chem.* **2018**, 37 (6), 1523–1534.
- (8) Ognard, J.; Barrat, J.-A.; Chazot, A.; Alavi, Z.; Salem, D. B. Gadolinium footprint: Cradle to cradle? *J. Neuroradiol.* **2020**, *47*, 247–249.
- (9) Martino, C.; Byrne, M.; Roccheri, M. C.; Chiarelli, R. Interactive effects of increased temperature and gadolinium pollution in Paracentrotus lividus sea urchin embryos: a climate change perspective. *Aquat. Toxicol.* **2021**, 232, No. 105750.
- (10) Brünjes, R.; Hofmann, T. Anthropogenic gadolinium in freshwater and drinking water systems. *Water Res.* **2020**, *182*, No. 115966.
- (11) Kümmerer, K.; Helmers, E. Hospital effluents as a source of gadolinium in the aquatic environment. *Environ. Sci. Technol.* **2000**, 34 (4), 573–577.
- (12) Künnemeyer, J.; Terborg, L.; Meermann, B.; Brauckmann, C.; Möller, I.; Scheffer, A.; Karst, U. Speciation analysis of gadolinium chelates in hospital effluents and wastewater treatment plant sewage by a novel HILIC/ICP-MS method. *Environ. Sci. Technol.* **2009**, 43 (8), 2884–2890.
- (13) Hatje, V.; Bruland, K. W.; Flegal, A. R. Increases in Anthropogenic Gadolinium Anomalies and Rare Earth Element Concentrations in San Francisco Bay over a 20 Year Record. *Environ. Sci. Technol.* **2016**, *50* (8), 4159–4168.
- (14) Cheisson, T.; Schelter, E. J. Rare earth elements: Mendeleev's bane, modern marvels. *Science* **2019**, *363* (6426), 489–493.
- (15) Torkaman, R.; Torab-Mostaedi, M.; Safdari, J.; Moosavian, M. A. Kinetics of gadolinium extraction with D2EHPA and Cyanex301 using single drop column. *Rare Metals* **2016**, 35 (6), 487–494.
- (16) Xie, F.; Zhang, T. A.; Dreisinger, D.; Doyle, F. A critical review on solvent extraction of rare earths from aqueous solutions. *Miner. Eng.* **2014**, *56*, 10–28.
- (17) Benedetto, J. S.; Ciminelli, V. S. T.; Neto, J. D. Comparison of Extractants in the Separation of Samarium and Gadolinium. *Miner. Eng.* **1993**, *6* (6), 597–605.
- (18) Arshi, P. S.; Vahidi, E.; Zhao, F. Behind the Scenes of Clean Energy: The Environmental Footprint of Rare Earth Products. ACS Sustainable Chem. Eng. 2018, 6 (3), 3311–3320.
- (19) Hidayah, N. N.; Abidin, S. Z. The evolution of mineral processing in extraction of rare earth elements using liquid-liquid extraction: A review. *Miner. Eng.* **2018**, *121*, 146–157.
- (20) Hovey, J. L.; Dittrich, T. M.; Allen, M. J. Coordination chemistry of surface-associated ligands for solid-liquid adsorption of rare-earth elements. *J. Rare Earths* **2023**, *41* (1), 1–18.
- (21) Dong, Z.; Mattocks, J. A.; Deblonde, G. J.; Hu, D.; Jiao, Y.; Cotruvo, J. A., Jr.; Park, D. M. Bridging Hydrometallurgy and

- Biochemistry: A Protein-Based Process for Recovery and Separation of Rare Earth Elements. ACS Cent. Sci. 2021, 7 (11), 1798–1808.
- (22) Gupta, N. K.; Gupta, A.; Ramteke, P.; Sahoo, H.; Sengupta, A. Biosorption-a green method for the preconcentration of rare earth elements (REEs) from waste solutions: A review. *J. Mol. Liq.* **2019**, 274, 148–164.
- (23) Hu, Y.; Florek, J.; Lariviere, D.; Fontaine, F. G.; Kleitz, F. Recent Advances in the Separation of Rare Earth Elements Using Mesoporous Hybrid Materials. *Chem. Rec.* **2018**, *18* (7–8), 1261–1276.
- (24) An, S.; Ranaweera, R.; Luo, L. Harnessing bubble behaviors for developing new analytical strategies. *Analyst* **2020**, *145* (24), 7782–7795
- (25) Gantt, B.; Meskhidze, N. The physical and chemical characteristics of marine primary organic aerosol: a review. *Atmos. Chem. Phys.* **2013**, *13* (8), 3979–3996.
- (26) Wilson, T. W.; Ladino, L. A.; Alpert, P. A.; Breckels, M. N.; Brooks, I. M.; Browse, J.; Burrows, S. M.; Carslaw, K. S.; Huffman, J. A.; Judd, C.; Kilthau, W. P.; Mason, R. H.; McFiggans, G.; Miller, L. A.; Najera, J. J.; Polishchuk, E.; Rae, S.; Schiller, C. L.; Si, M.; Temprado, J. V.; Whale, T. F.; Wong, J. P.; Wurl, O.; Yakobi-Hancock, J. D.; Abbatt, J. P.; Aller, J. Y.; Bertram, A. K.; Knopf, D. A.; Murray, B. J. A marine biogenic source of atmospheric ice-nucleating particles. *Nature* 2015, 525 (7568), 234–238.
- (27) Cao, Y.; Lee, C.; Davis, E. T. J.; Si, W.; Wang, F.; Trimpin, S.; Luo, L. 1000-Fold Preconcentration of Per- and Polyfluorinated Alkyl Substances within 10 minutes via Electrochemical Aerosol Formation. *Anal. Chem.* **2019**, *91* (22), 14352–14358.
- (28) Niendorf, H. P. Gadolinium-DTPA: a new contrast agent. Bristol Med.-Chir. J. 1988, 103 (2), 34.
- (29) Tweedle, M. F.; Hagan, J. J.; Kumar, K.; Mantha, S.; Chang, C. A. Reaction of gadolinium chelates with endogenously available ions. *Magn. Reson. Imaging* **1991**, *9* (3), 409–415.
- (30) Hovey, J. L.; Dardona, M.; Allen, M. J.; Dittrich, T. M. Sorption of rare-earth elements onto a ligand-associated media for pH-dependent extraction and recovery of critical materials. *Sep. Purif. Technol.* **2021**, 258, No. 118061.
- (31) Barge, A.; Cravotto, G.; Gianolio, E.; Fedeli, F. How to determine free Gd and free ligand in solution of Gd chelates. A technical note. *Contrast Media Mol. Imaging* **2006**, *1* (5), 184–188.
- (32) Ranaweera, R.; An, S.; Cao, Y.; Luo, L. Highly efficient preconcentration using anodically generated shrinking gas bubbles for per- and polyfluoroalkyl substances (PFAS) detection. *Anal. Bioanal. Chem.* **2023**, 415 (18), 4153–4162.
- (33) Hermann, P.; Kotek, J.; Kubicek, V.; Lukes, I. Gadolinium(III) complexes as MRI contrast agents: ligand design and properties of the complexes. *Dalton Trans.* **2008**, No. 23, 3027–3047.
- (34) Shmaefsky, B. Artificial Urine for Laboratory Testing Revisited. Am. Biol. Teach. 1995, 57 (7), 428-430.
- (35) Bénazeth, S.; Purans, J.; Chalbot, M. C.; Nguyen-Van-Duong, M. K.; Nicolas, L.; Keller, F.; Gaudemer, A. Temperature and pH Dependence XAFS Study of Gd(DOTA)(-) and Gd(DTPA)(2)(-) Complexes: Solid State and Solution Structures. *Inorg. Chem.* 1998, 37 (15), 3667–3674.
- (36) Moulin, C.; Amekraz, B.; Steiner, V.; Plancque, G.; Ansoborlo, E. Speciation studies on DTPA using the complementary nature of electrospray ionization mass spectrometry and time-resolved laser-induced fluorescence. *Appl. Spectrosc.* **2003**, *57* (9), 1151–1161.
- (37) Li, X.; Luo, L.; Crooks, R. M. Low-voltage paper isotachophoresis device for DNA focusing. *Lab Chip* **2015**, *15* (20), 4090–4098.
- (38) Luo, L.; Li, X.; Crooks, R. M. Low-voltage origami-paper-based electrophoretic device for rapid protein separation. *Anal. Chem.* **2014**, 86 (24), 12390–12397.
- (39) Djurdjevic, P.; Jelic, R.; Joksovic, L.; Lazarevic, I.; Jelikic-Stankov, M. Study of Solution Equilibria Between Gadolinium(III) Ion and Moxifloxacin. *Acta Chim. Slov.* **2010**, *57* (2), 386–397.
- (40) Mullica, D. F.; Lok, C. K. C.; Perkins, H. O.; Benesh, G. A.; Young, V. The X-Ray Photoemission Spectra of Nd(Oh)(3), Sm(Oh)

(3), Eu(Oh)(3) and Gd(Oh)(3). J. Electron Spectrosc. Relat. Phenom. 1995, 71 (1), 1–20.